INTERNATIONAL ATOMIC ENERGY AGENCY
UNITED NATIONS EDUCATIONAL, SCIENTIFIC AND CULTURAL ORGANIZATION

INTERNATIONAL CENTRE FOR THEORETICAL PHYSICS
34100 TRIESTE (ITALY) - P.O.B. 586 - MIRAMARE - STRADA COSTIERA 11 - TELEPHONE: 2240-1
CABLE: CENTRATOM - TELEX 460892-I

H4.SMR/210 - 46

SPRING COLLEGE ON PLASMA PHYSICS

(25 May - 19 June 1987)

THE PHYSICS OF FIELD-REVERSED CONFIGURATION PLASMAS

L.C. Steinhauer
Spectra Technology, Inc.
Bellevue, WA 98004
U.S.A.

THE PHYSICS OF FIELD-REVERSED CONFIGURATION PLASMAS

Loren C. Steinhauer
Spectra Technology, Inc.
2755 Northup Way
Bellevue, WA 98004

This paper was prepared for presentation at:

Spring College on Plasma Physics
International Centre for Theoretical Physics
Trieste, Italy; 25 May - 19 June 1987

29 May 1987

THE PHYSICS OF FIELD-REVERSED CONFIGURATION PLASMAS

Loren C. Steinhauer
Spectra Technology, Inc.
2755 Northup Way
Bellevue, WA 98004

ABSTRACT

A review is given of field-reversed configuration (FRC) plasma physics. The historical background on the emergence of FRCs as a fusion confinement concept is discussed along with the present state of progress. FRC physics is organized into major topics, formation, equilibrium, macrostability, and transport, each of which is reviewed. Special attention is devoted to the internal tilting instability because of its current importance in FRC development. An annotated bibliography of key literature on FRC research is offered in the final section.

I. INTRODUCTION

The field-reversed configuration (FRC) is a subclass of magnetic fusion confinement concepts known as compact toroids. Compact toroids are unique among closed magnetic field line systems in that they have no walls or coils passing through the center of the toroid, hence the designation "compact". FRCs are particularly unusual because they have no appreciable toroidal magnetic field. Other toroidal confinement systems require the toroidal magnetic field component to be comparable to, or much greater than the poloidal field in order to achieve stability of the plasma. Indeed, the stability of the FRC despite its lack of a toroidal magnetic field is one of its most intriguing aspects.

Figure 1 is a schematic diagram of a FRC emphasising its magnetic characteristics. The configuration is composed of a bundle of closed poloidal magnetic field lines enclosed by the separatrix, which is surrounded by open field lines. In most FRCs the external magnetic field is supported by a cylindrical coil which acts as a surface of constant magnetic flux. The plasma on closed field lines is represented in the figure by the shaded region. Not shown is the important but relatively thin edge layer located just outside the separatrix. The edge layer connects to spindle-like jet regions extending out the ends of the coil.

A. Historical Perspective on FRCs

Today, most FRCs are generated in theta pinch devices, which are one-turn cylindrical coils. Using a high-voltage capacitive power supply and associated circuitry, the magnetic field is given a rapid initial rise followed by a long, relatively slow decay. Research on theta pinches dates from the late 1950s. They were appealing for nuclear fusion because the rapidly rising magnetic field shock-heats the plasma, producing keV ion temperatures. The early research emphasised maximising neutron production; therefore high magnetic fields (up to 100 kG) were used to reach the

highest possible temperatures and densities. Early theta pinch research employed what is known today as "second half-cycle operation" in which the magnetic field is first allowed to "ring" through a half cycle in what is designated the "reversed" direction. This facilitates the initial ionization of the plasma. During the second half cycle as the magnetic field begins to rise in the "forward" direction, the newly ionized plasma is rapidly compressed and heated. Theoretical studies in the early 1960s recognized the possibility of closed field lines arising from the reversed magnetic flux imbedded in the plasma during the first half cycle.

There were, however, three major problems with "field-reversed theta pinch" plasmas. 1) The reversed magnetic flux seemed to be quickly annihilated; this is not surprising because of the high magnetic field and correspondingly strong radial compression produced a rather small plasma radius (often less than a centimeter). 2) The plasma was subject to a rotational instability which produced a fast-growing elliptical distortion which disrupted the plasma. 3) The elongated (high length-to-diameter ratio) plasma was subject to a tearing instability, which tore the plasma into two or more small parts. These problems prevented the serious development of "field-reversed theta pinch" plasmas as a confinement concept during the 1960s.

Positive results from a landmark experiment at Garching in 1970 led to a reconsideration of field-reversed theta pinches (Eberhagen, 1971). This experiment used lower magnetic fields, avoiding the overcompression of the earlier experiments. By careful attention to external magnetic field uniformity, the plasmas were stable to the tearing mode. The rotational instability appeared, but only after times on the order of the decay of the configuration. Soon after, experiments on a series of devices were initiated at the Kurchatov Institute. These also used low compressions but added innovative techniques to control the formation, such as independent control coils at the ends of the main coil. Oddly, the rotational instability was not observed. Detailed information on these experiments was first reported in 1978 (Es'kov, 1978) at which time the term "compact

toroid" was coined. These successes motivated the initiation of what later became known as the FRX series of devices at Los Alamos in 1976, several devices in Japan (about 1980), and the TRX series at Spectra Technology (1981). The first thorough and comprehensive reporting of observations on such plasmas was in 1981 (Armstrong, 1981), in which the designation "field-reversed configuration" (FRC) was first used.

B. Motivation for FRC Research

FRC plasmas physics is inherently interesting because of the unusual configuration and properties. Laboratory FRCs can be used to study space plasma phenomena such as tearing in the Earth's magnetotail. However, the primary factor motivating FRC research is its attractiveness as a nuclear fusion concept. The configuration is remarkably simple in several ways, beginning with the straight cylindrical geometry with no center column. It requires only one magnetic field component (poloidal). Thus, unlike other toroidal confinement concepts, there is no need for a toroidally-shaped confinement chamber or interlinking coils. A second attribute of the FRC is its efficient use of magnetic energy. With no toroidal field, the plasma pressure equals the magnetic field pressure, so that the magnetic field required for a given plasma pressure is relatively low. Consequently the magnet system design is simplified because of lower magnetic fields, reduced coil stresses, and smaller magnetic energy storage. Third, since the plasma is contained in an "open" cylindrical chamber, it is possible to move, or "translate" the FRC axially along the external magnetic field. This attribute makes it possible to first form the FRC in one chamber, and then translate it to another for the fusion reaction. Such a separation of functions allows the conflicting requirements of plasma formation and nuclear fusion burn to be handled in separate parts of the reactor. Finally, the edge layer connecting to the exhaust jets provides a natural divertor, without the requirement of special divertor coils.

C. Basic Characteristics of Present-Day FRC Plasmas

Typical FRC parameters in recent experiments are listed in Tab. I. FRCs have the highest value of $\langle\beta\rangle \equiv \langle p\rangle/B_e^2/2\mu$ (B_e is the "external" magnetic field supplied by the coil), and density of any of the major magnetic fusion concepts. The plasma volumes are the smallest, by far, among major fusion concepts. Although the confinement times are not very long, the thermal diffusivity, χ_E (which measures the effectiveness of energy confinement), is comparable to other fusion concepts. Because of the high-density, the $n\tau$ product is unusually high for such a small plasma size. Most FRC experimental research is carried out on theta pinch devices. Table II lists the key parameters of the active theta pinches, showing the main coil dimensions, peak magnetic field, and rise time. Also shown are the parameters of the translation chamber, where applicable. Not listed in Tab. II are non-theta pinch FRC devices,

Despite their uniqueness, FRC plasmas share certain common features with other magnetic confinement concepts. Although its superficial appearance is cylindrical, the FRC is a genuine toroidal configuration with closed magnetic field lines, like the tokamak, reversed-field pinch (RFP), stellarator, and spheromak. Plasma confinement in a FRC is by the pinch effect, in which substantial plasma currents supply the confining force, as is the case for the tokamak, RFP, and spheromak. Among these pinch-effect concepts, the FRC has the highest current density (highest electron drift speed). A important feature of an FRC is the edge layer located just outside the separatrix. In common with mirror and cusp plasmas, the edge layer exhibits strong magnetic mirroring and electrostatic effects. FRCs have a significant rotational motion, as now appears to be the case in many tokamak experiments. Since FRCs have no toroidal field, the internal magnetic field is low in much of the plasma interior, leading to strong ion kinetic effects; this is similar to the old Astron concept, and has some analogies in mirror physics.

D. Organisation of FRC Physics Topics

FRC plasma physics can be organised into a number of subtopics, four of which will be discussed here. These areas are placed into a hierarchy of timescales, arranged from short to long. The first topic is formation, during which the plasma is generated and formed into a FRC. In theta pinches at least, this process takes place on a timescale between the radial Alfven time (r_s/v_A), and the axial Alfven time (ℓ_s/v_A). Alternative formation techniques, called "slow sources", are currently being investigated, which involve much longer timescales. In such devices, the formation process is strongly influenced by macrostability and global transport issues, which is not generally the case for formation in a theta pinch. FRC formation in a theta pinch is reviewed in Sec. II.

The second topic of FRC physics is equilibrium, which describes a stationary state lasting for timescales longer than the axial Alfven time. Equilibrium and the associated topic of translation are discussed in Sec. III. The third topic, macrostability, describes a property of the equilibrium state, and therefore spans timescales longer than the axial Alfven time. The prefix macro indicates that large-scale, or global modes are in view rather than small-scale (length scales less than an ion gyroradius). global modes generally affect the integrity of the entire configuration whereas small scale modes only affect the transport rates. Macrostability is discussed in Sec. IV where special attention is given to the internal tilting mode, regarded by many as the most dangerous instability. The fourth topic is transport, covering both the question of transport mechanism (including microstability), and issue of how the overall configuration evolves in response (sometimes called "global transport"). Transport has the longest timescale, the diffusive time $\mu r_s^2/8\langle\eta_\perp\rangle$. FRC transport is discussed in Sec. V. The final section, VI, is an annotated bibliography of selected papers.

There are other important FRC physics issues of particular importance to the fusion reactor application, which are not covered here. These

include reactor-relevant sources (an issue with strong technology as well as physics implications), plasma heating to fusion ignition temperatures, steady-state maintenance of a FRC plasma, and burning plasma physics. Although these topics are important, very little research with immediate relevance to FRCs has been done.

II. FORMATION

The most common method of forming a FRC is in a theta pinch. Other methods, which might be technologically more attractive for a fusion reactor (coaxial slow source and rotamak) are not discussed here.

FRCs are formed in theta pinches by rapidly reversing the external field and trapping a portion of the preimposed bias magnetic flux. Connection of the imbedded bias flux to an equal amount of oppositely directed external flux produces a closed field-line toroidal configuration. The basic steps in this process are illustrated in Fig. 2, which shows the two-dimensional (r,s) magnetic flux contours during formation. A gas fill is first preionised in the presence of a bias magnetic field (step 0). The magnetic field at the coil is rapidly reversed. Initially, as the field at the wall decreases in magnitude, the plasma is driven outward by the pressure of the imbedded magnetic field. As the field at the wall reverses and rises to a magnitude exceeding the internal field, the plasma flow toward the wall is stopped and reversed. The subsequent "liftoff" ends the field-reversal phase (step 1). After liftoff, the plasma is radially compressed and heated by the rising magnetic field. Substantial ohmic heating also occurs during this phase as some of the internal magnetic flux is dissipated (step 2). The initiation of the next stage, axial contraction (step 3), depends on the geometry and control coils at the end of the main coil. (Fig. 2 shows the particular case of a steady coil which produced a magnetic cusp with the bias field). Finally, after some axial and radial bouncing motion, a quiescent equilibrium is reached (step 4).

Considerable study has been devoted to the formation of FRCs in theta pinches. Indeed, much of the work on the Soviet and TRX series of devices has been devoted to understanding formation phenomena, and finding improved techniques for the formation. The techniques employ special controls at the ends of the main coil, special preionisation methods, or multipole windings along the chamber wall. These methods are quite sophisticated and

are not discussed here. The discussion that follows focuses instead on generic aspects of formation, including analysis of the field-reversal phase, and aspects of the radial and axial compressions. It concludes with a review of issues that are not well understood.

A. Field-reversal Phase

Field reversal is the phase between the firing of the main coil and liftoff when the rising external field drives the plasma off the wall. Field reversal determines how much imbedded reversed flux is retained by the plasma at liftoff. This flux is customarily described described in terms of B_{L0}, defined as the reversed flux divided by the cross-sectional area inside the chamber wall, πr_w^2. The magnitude of B_{L0} has a strong affect on the subsequent dynamics and plasma heating intrinsic to the formation process.

Field-reversal has been examined theoretically by two methods, a one-dimensional MHD code and a quasianalytic MHD model (Steinhauer, 1985). The key assumption of the quasianalytic model is that the outward flow of plasma and magnetic flux produces a thin current sheath near the wall, which can be analyzed using a quasi steady-state assumption. The model predicts that the efficiency of flux retention during field reversal (B_{L0} divided by the initial bias field, B_o) is given by

$$B_{L0}/B_o = \left[1 + 3\lambda^{1/2}\left(1/\eta_t - 1\right)^{2/5} \right]^{-1} \qquad [1a]$$

$$\lambda \equiv \frac{B_o^2/2\mu n_o}{eV_c/2\pi N_t} \qquad [1b]$$

where η_t is the energy transfer efficiency from the capacitor bank to the chamber volume, proper, n_o is the initial filling density, V_c is the initial capacitor voltage, and N_t is the number of turns in the theta pinch coil. The parameter λ expresses the ratio of two energies, the initial

magnetic energy per ion divided by the energy imparted by acceleration across an electrostatic potential, $V_c/2\pi N_t$. Figure 3 indicates a good comparison between experiment, time-dependent MHD computations, and the analytic model. Evidently, lower voltages lead to reduced flux retention, but with a relatively weak dependence. Equally important is the coupling of the power supply to the plasma tube, measured by η_t. Small external inductance and a coil closely coupled to the tube (r_c only slightly larger than r_w) gives η_t a value near unity, resulting in good flux retention.

B. Radial and Axial Compression of the Plasma

The post liftoff behavior of the plasma has been analyzed by global analytic models and by 2D-MHD computations. The analytic models have highlighted the key thermodynamic elements such as the importance of dissipative heating. The computations have corroborated the analytic models and given numerous insights into detailed phenomena observed in experiments.

1. Global Analytic Modelling of FRC Formation.

The post liftoff behavior of the plasma has been described using a global thermodynamic model (Steinhauer, 1983). A simplified version of this analysis (Hoffman, 1986) is summarized here. The loss of flux after liftoff is assumed to be governed by the a rapid relaxation that reduces the drift parameter, v_D/v_i (electron drift speed / ion thermal speed) to a fixed value, which is empirically determined. In practice, the relaxation results from fast-growing microinstabilities characteristic of theta pinch implosions. Since the axial contraction broadens the plasma radially and reduces the drift parameter, the relaxation condition is applied to the radial compression phase.

Using this formulation, the equilibrium poloidal flux divided by the liftoff flux is

$$\phi_p/\phi_{L0} \cong \nu\tilde{N}^{1/2}\left(500 + \nu^4\tilde{N}^2\right)^{-1/4} \qquad [2a]$$

$$\tilde{N} \equiv \mu e^2 n_o r_w^2/2m_i \qquad [2b]$$

where ν is the drift parameter relaxation constant, and n_o is the initial average plasma density. Evidently, a lower relaxation constant causes more flux loss, and a higher initial density causes less. Figure 4 is a plot of the poloidal flux (normalized by the tube cross-sectional area) versus the initial filling pressure (which is related to n_o). Evidently a value of ν = 0.35 gives a best fit to the data shown.

The strong heating intrinsic to the formation process begins at liftoff. Several phenomena contribute to the heating: 1) radial shock heating by the magnetic "piston" (as in ordinary theta pinches); 2) adiabatic compression heating by the rising magnetic field; 3) resistive heating of the internal magnetic field is dissipated; and 4) dissipation of axial compression energy. These are taken into account in the global thermodynamic model, where the process is regarded as a series of distinct steps (as described earlier), linked together by global conservation laws. This leads to a prediction of the temperature in the subsequent equilibrium,

$$T_e+T_i = \frac{4B_e^{4/5}}{5\mu n_o k}\left(f_p B_{L0}^{6/5} + 0.32 f_s B_{GN}^{6/5}\right) \qquad [3]$$

where B_e is the external field in the equilibrium, and B_{GN} is the critical magnetic field (Green, 1966),

$$B_{GN} \equiv E_\theta\left(\mu m_i n_o\right)^{1/4} \qquad [4]$$

The factors f_p, and f_s are typically 1.0 and 0.45, respectively (more general expressions are given by Hoffman, 1986). The B_{GN} part of (4) represents radial shock heating which is the predominant factor in ordinary theta pinches. The B_{L0} par represents the contribution of resistive

heating and dissipation of the axial contraction energy. Evidently, the ratio B_{L0}/B_{GN} measures the importance of effects associated with the bias field; if this ratio is comparable to unity or greater, then substantially more heating is produced than in an ordinary (no bias) theta pinch. Figure 5 is a plot of the temperature as a function of filling pressure, showing a comparison between the theory and experimental observations. Note the substantial increase in heating because of the bias field.

2. 2D-MHD Computation of FRC Formation.

Two-dimensional MHD computations have served to confirm the results of the global models. Their most important role, however, has been in explaining detailed experimental phenomena (Milroy, 1982). This latter role has been essential in view of the several variations in the formation technique that have been tested experimentally. Figure 2, introduced earlier, represents one variation of "programmed formation" (Belikov, 1982).

Other more generic phenomena have been explored in detail, including details of the axial contraction dynamics (initiation, speed of the contraction wave, magnitude of the overbounce). Numerical computations have been used to infer the poloidal flux (after the radial compression phase) from the strength of the axial contraction waves (Milroy, 1987). The same study explored the importance of parallel viscosity, $\mu_\parallel$, in damping the axial contraction dynamics. Since $\mu_\parallel \propto T_i^{5/2}$, the viscosity of the plasma is extremely sensitive to the temperature, which is inversely proportional to the initial density (see eq. 3). In the TRX-2 experiment, initial fill pressures less than 10 mTorr ($n_o \leq 7 \times 10^{14}$ cm^{-3}) led to extremely viscous plasma behavior, i.e. a strongly damped axial compression wave, and no overbounce oscillations. Moreover, the transition to nonviscous behavior was quite abrupt above 10 mTorr.

C. Unresolved FRC Formation Issues

There are several unanswered questions about FRC formation. One unknown is the resistivity mechanism during the radial compression, during which most of the dissipation occurs. It may be that the same microturbulence mechanisms occur as in a theta pinch implosions. Oddly, even for relatively slow compressions (e.g. on TRX-2 where radial shock heating is minimal) the observed ion temperature can substantially exceed the electron temperature. Evidently the turbulence deposits a very large share of the energy directly with the ions.

The most important unanswered issues pertain to formation pathologies of unclear origin. The manifestation of these pathologies is the ability to form long-lived FRCs (more than 20 μs or so) only within a fairly limited "operating window". The operating window can be described empirically as follows. 1) Fill pressure: too low filling pressure leads to inadequate preionization; too high filling pressure leads to either too violent axial dynamics, or to too long equilibria (which try to extend beyond the ends of the main coil). 2) Formation technique: the programmed formation methods described earlier are much more successful at achieving reproducible formation (especially at high bias magnetic field), than methods based on tearing reconnection (which do not use the "plug coil" shown in Fig. 2). 3) Bias field: too high bias field leads to violent axial dynamics. 4) Preionization (PI): quality of the PI plasma, especially azimuthal symmetry is necessary, especially at high bias field. 5) Device size: formation in larger devices becomes increasingly difficult.

Two unifying factors characterize these empirical observations. First, azimuthal symmetry is important for successful formation; hence the need for PI quality and the programmed formation method (which produces highly symmetric reversed-to-forward field line connection at the ends of the main coil). Second, violent axial compression dynamics are to be avoided; hence the difficulties at higher filling pressure, high bias field (which causes strong axial dynamics), and large device size (which retains the bias flux more efficiently and thus is more prone to strong axial

dynamics). It may be that a FRC that suffers too strong axial overcompression is unstable to tilting; the presence of azimuthal asymmetries may drive the tilt more strongly. Several effects which would mitigate the overcompression are under study, including ion viscosity, control coil modifications, and adjusted timing of the axial contraction.

III. EQUILIBRIUM

FRC equilibria are examined with emphasis on simple analytical descriptions. A short discussion of translation is also given.

A. Characteristics of FRC Equilibria.

The basic definition of a FRC is a toroidal magnetic configuration with no toroidal magnetic field. Consequently, a FRC has no rotational transform and no shear. If the z axis coincides with its main axis, then there are only radial and axial magnetic field components, and the current density is purely azimuthal. It might be added that most FRCs (those formed in theta pinches) are elongated, as portrayed in Fig. 1, i.e. the elongation, $\ell_s/2r_s$ is somewhat larger than unity.

Equilibria are governed by the force balance equation,

$$\nabla p - \rho\Omega^2 r\,\hat{r} = \vec{j} \times \vec{B} \qquad [5]$$

where Ω is the local rotational frequency. Almost all equilibrium analyses have ignored the rotational effect (taking $\Omega = 0$). In the discussion that follows, no rotation is assume except where otherwise noted. The magnetic field in a FRC can be expressed in terms of a magnetic stream function, ψ.

$$\vec{B} = \frac{\hat{\theta}}{r} \times \nabla\psi \qquad [6]$$

Elongated FRC equilibria confined in straight, constant-flux magnets have remarkably simple properties. These properties, some of which were demonstrated in a landmark paper (Armstrong, 1981), greatly facilitate equilibrium analysis. 1) The separatrix radius at the midplane of symmetry and the radius of the magnetic axis (r=R, z=0, sometimes called the magnetic field null, or the "0 point"), are in a fixed ratio,

$$r_s^2/R^2 = 2 \qquad [7]$$

This property follows from the continuity between the "reversed" and "forward" parts of the closed magnetic flux lines. 2) A very simple algebraic expression relates the local pressure and axial magnetic field,

$$p + \frac{B_z^2}{2\mu} = \text{const} = \frac{B_e^2}{2\mu} \qquad [8]$$

This property follows from the fact that $B_r << B_z$ everywhere except near the ends of an elongated FRC. 3) The average value of $\beta \equiv p/(B_e^2/2\mu)$ taken over the midplane cross-section inside the separatrix is governed by

$$\langle\beta\rangle = 1 - r_s^2/2r_c^2 \qquad [9]$$

This property, sometimes called the "average-β relation" follows from a force balance calculation inside the straight coil and between plane surfaces at the midplane and beyond one end of the FRC. 4) The previous properties lead to an approximate expression for the poloidal flux (2π times the magnetic stream function at the magnetic null),

$$\phi_p \cong B_e r_s^2/r_c \qquad [10]$$

which is a good approximation for "reasonable" equilibria. The particle inventory (total number of ions inside the separatrix) is approximately

$$N \cong \frac{\pi r_s \ell_s}{2} \int n d\ell \qquad [11]$$

where $\int n d\ell$ is the integrated density across the diameter at the midplane, which is routinely measured by interferometric techniques. The plasma energy is

$$E_p = \frac{3}{2}\left(1 - \frac{r_s^2}{2r_c^2}\right)\frac{B_e^2}{2\mu}\pi r_s^2 \ell_s \qquad [12]$$

These simplified expressions have facilitated both the measurement of global transport (see Sec. V) and the construction of several one dimensional (r) approximations of the equilibrium which have been very useful in transport modeling.

In addition to the above approximate properties, there are exact analytical expressions of equilibria. The most widely used is the Hill's vortex equilibrium, for which the magnetic stream function is given by,

$$\psi = \frac{B_a r^2}{2}\left(1 - \frac{r^2}{r_s^2} - \frac{4z^2}{\ell_s^2}\right) \qquad [13]$$

which holds inside of the elliptical separatrix, $(r/r_s)^2 + (2z/\ell_s)^2 = 1$. An analytical description of rotating FRC equilibria has also been used (Clemente, 1983) which reduces to the Hill's vortex in the limit, $\Omega \to 0$.

A number of numerical computations of FRC equilibrium have been reported. These represent solutions to the Grad-Shafranov equation; in the FRC case (no toroidal field) this is

$$r\frac{\partial}{\partial r}\left(\frac{1}{r}\frac{\partial \psi}{\partial r}\right) + \frac{\partial^2 \psi}{\partial z^2} = -\mu r^2 p'(\psi) \qquad [14]$$

These computations have served mainly to confirm the analytical properties described earlier. In addition some specialized effects have been examined, including special coil shapes, auxiliary coils, compression, low-elongation, and the influence of the edge-layer plasma. One paper in particular has made a comparison between computation and experimental observations of equilibria (Spencer, 1985).

B. Translation of FRCs

Translation studies have been reported from the OCT and FRX-C/T devices (Rej, 1986). In these experiments, an FRC is formed in a theta pinch, and launched into a steady state axial "guide field". The launching is accomplished by means of a slight taper in the theta pinch coil or by a mirror coil at one end of the main coil. Two-dimension MHD computations have been helpful in interpreting the experimental observations on such matters as the translational speed of the FRC, the kinetic energy lost in bouncing off a mirror, structural distortions in bouncing off the mirror, and the viscous behavior of the plasma (Rej, 1986).

IV. MACROSTABILITY

Since the favorable results from the landmark experiment at Garchirg (Eberhagen, 1971) resistive instabilities, such as tearing modes, have not been regarded as a major problem in FRCs. Indeed, it appears that such modes are easily stabilized by a conducting wall (Berk, 1982). This section therefore focuses on nonresistive modes. Two macroscopic modes have been particularly important in FRC research, the rotational instability and the internal tilt instability.

A. Rotational Instability

The common trademark of FRC plasmas from the earliest days has been the rotational instability. In typical experiments, the FRC remains more or less axisymmetric for times ranging from 15 to 70 μs (the so-called "stable time"), after which a rotating elliptical distortion appears, as viewed from the end. The distortion grows rapidly into a highly distended propeller-like figure which rubs against the wall and disrupts the confinement. There are instances in which the mode doesn't appear, e.g. in some rapidly-decaying FRCs, and unpredictably on other occasions. However, it is safe to say that the mode is essentially universal in FRCs of interest.

Considerable attention was devoted to understanding two issues: 1) the cause of the spinup, and 2) the rotational stability threshold. The earliest spinup mechanism to be suggested (Eberhagen, 1971) is that particles lost at the separatrix have a preferential angular momentum. This led to the prediction that the instability would appear on a timescale comparable to the particle confinement time, τ_N (Barnes, 1979). Later another mechanism was investigated (Steinhauer, 1981). The edge-layer plasma is rotated by the shorting of the radial electric fields in the same way as with ordinary theta pinches. Subsequently, by shear viscosity, the plasma inside the separatrix is also caused to rotate. Subsequent

experimerts (Aso, 1982) and theory (Harned, 1984) suggested that both mechanisms contribute to the spinup, although the relative role of each has not been well characterised.

Likewise the rotational instability threshold received considerable attention. Early work based on a finite-Larmor-radius (FLR) expansion predicted that the stability threshold for Ω is comparable to the diamagnetic drift frequency, $\Omega_D \equiv \nabla p_i/renB$, which is the case for ordinary theta pinches. However, the FLR expansion is not strictly valid in a FRC because the Larmor radius becomes very large near the magnetic field null. A hybrid computation (kinetic ions and fluid electrons) showed that while lower Ω reduces the growth rate, it is unstable for any nonzero rotation (Harned, 1983).

However, an achievement in 1982 rendered moot much of the discussion about spinup mechanism and stability threshold. It was demonstrated on the PIACE experiment that the rotational mode is stabilized by the application of a modest multipole magnetic field (Ohi, 1983). Within one year, this important result was confirmed on the TRX-1 and FRX-C experiments. Later an MHD theory was developed (Ishimura, 1984), yielding the following stability threshold for quadrupoles,

$$B_q^2/2\mu \geq (\pi^2/2)\, \rho r_s^2 \qquad [15]$$

Where B_q is the peak quadrupole field magnitude at the separatrix.

Since then detailed comparisons have been made between (15) and experimental observed thresholds. It has been found that the observed threshold for B_q is a factor of 1.5 to 4 lower than predicted by theory. Since kinetic (non fluid-like) phenomena should affect the stability, a hybrid computation (kinetic ions, cold fluid electrons) has been done. Figure 6 shows both hybrid theory and experimental observations of the rotational mode (Rej, 1986). Qualitative agreement is clearly seen: for low B_q (or the corresponding quadrupole current) the strength of the

instability is unaffected. However at a certain level, the mode is quite abruptly suppressed. Hidden in Fig. 6 (since different quantities, B_q and I_q, are used to measure the quadrupole strenght), is the fact that a factor of two discrepancy remains. This, however, is an improvement over the MHD model which is a factor of four too high in this instance. The cause of the remaining discrepancy is not known.

B. Internal Tilt Instability

The single area of FRC research receiving the most attention in recent years is the internal tilt instability. This is analogous to the effect by which a current-carrying ring immersed in an externally-generated magnetic field tends to turn over if the ring current field opposes the external field. The tilt instability first came to prominence as a result of a landmark paper (Rosenbluth, 1979). Although this paper dealt with spheromaks, its conclusions were later confirmed to apply to FRCs as well. One of the conclusions was that an elongated configuration is unstable to an internal tilt mode, i.e. the normal component of the displacement vector field, $\vec{\xi}$, vanishes at the separatrix. Consequently, the tilt mode in an elongated configuration cannot be stabilized by a closely-fitting conducting wall.

Since the original paper, several analyses of the internal tilt mode have been made. For example, Schwarzmeier (1983) presented the results of two methods, a trial function approach and an initial value problem (linearized MHD). Results from the initial value problem approach indicated that the eigenfunction, $\vec{\xi}(\vec{r})$, has the following properties: 1) the displacement vectors are primarily axial in elongated configurations; 2) not only is the normal component of $\vec{\xi}$ small at the separatrix, but the magnitude of $\vec{\xi}$ is small on the entire $\psi = 0$ surface (including the separatrix and the main axis); and 3) the displacement function is incompressible, $\nabla\cdot\vec{\xi} = 0$, so that compressibility effects are unimportant. A range of equilibria were considered, from "elliptical" (Hill's vortex

like) to "racetrack" (relatively straight internal magnetic fields except very near the ends). From these calculations, one can infer the form of the internal tilt growth rate,

$$\gamma_{tilt} \simeq \frac{2B_e}{\ell_s(\mu m_i n)^{1/2}} \qquad [16]$$

where B_e is the external field. The growth rate is very rapid; $1/\gamma_{tilt}$ ranges from 1 to 5 μs in typical experiments. The nonlinear growth of the internal tilt was expected to produce localised antiparallel fields near the ends of the FRC (with associated high current densities). In a finite resistivity plasma, this would almost certainly lead to a tearing instability, opening up the internal field lines and causing the loss of confinement.

However, the remarkable fact is that there is no unambiguous experimental evidence for the internal tilt. Indeed, there are many examples where the configuration lifetime is in the range of 50 to 200 times $1/\gamma_{tilt}$. This stands in marked contrast to spheromak experience where the tilt is predicted by theory and clearly observed in experiment. Three explanations have been offered to resolve this intriguing anomaly. First, ion kinetic effects (finite orbit size) can have a strong stabilizing effect. It has been argued that if the growth rate is reduced enough, then present configuration lifetimes (set by the transport rates) are too short for instability growth to large magnitude. Second, the mode may be nonlinearly stabilised producing a static or dynamic equilibrium that is only moderately tilted. Third, stabilization may result from rotation (gyroscopic stabilization) or some other unidentified effect.

The second possibility was examined in recent computations with a fully nonlinear 3D-MHD code (Milroy, 1987). The results for one example are shown in Fig. 7. Evidently the internal tilt mode grows to large proportions without evidence of stabilization. At t = 50 μs, the tilt is nominally 90 degrees, producing a highly distorted internal magnetic

structure. Given finite resistivity, this configuration should tear open and lose confinement.

The discussions that follow address the other two suggested explanations for the nonobservance of tilting.

1. Kinetic effects on the internal tilting mode

Present day FRCs are highly kinetic, i.e. the ion orbit size is comparable to the minor radius. A parameter, s, has been defined to measure the importance of kinetic effects,

$$s \equiv \int_R^{r_s} \frac{r}{r_s} \frac{dr}{\rho_i} \simeq \frac{x_s}{5} \frac{R}{\rho_{io}} \qquad [17]$$

where ρ_i is the local ion gyroradius and ρ_{io} is the gyroradius based on the external field, B_e. In effect, s measures the number of real (local) gyroradii between the magnetic null and the separatrix. As $s \to \infty$ the behavior becomes MHD like (except in an increasingly small neighborhood of the field null), whereas it is highly kinetic for s of order unity or less. Present experiments, for which $0.5 < s < 2$, are clearly in the regime where kinetic effects are important.

Although there are several approaches the kinetic stability problem, the most work has been done using the Vlasov-fluid model (Barnes, 1986). This describes the ion species as collisionless and the electron species as a cold, massless fluid. A dispersion function was derived in which fluid and kinetic contributions were distinguished. The kinetic portions were calculated by a Monte Carlo method following a sample of the equilibrium orbits. The results reported to date have employed the MHD eigenfunction as a trial function (found earlier by an initial value code, Schwarzmeier, 1983). Ongoing work is attempting to find the self-consistent eigenfunction. Figure 8 shows the results of the Vlasov-fluid approach to date: the growth rate is normalized to the MHD ($s \to \infty$) limit. For present

experiments the growth rate is predicted to be reduced by a factor of ten or more.

One of the features of the Vlasov-fluid model is that it affects the growth rates but not the marginal stability conditions. Thus, if the internal tilt mode is MHD-unstable, the Vlasov-fluid model will likewise predict instability, albeit with a lower growth rate. Of course the Vlasov-fluid description does not include flows (such as ion rotation), finite electron pressure effects, or nonfluid like electric fields. It cannot be ruled out that a less restrictive kinetic model may reach full stabilization under some conditions.

Figure 8 illustrates one motivation for the LSX experiment, presently under construction at Spectra Technology. LSX, a large theta pinch (see Tab. II), is projected to achieve s = 8, for which kinetic stabilization effects will be much weaker. Based on transport estimates, s = 30 is needed for a FRC fusion reactor.

2. Other stabilization mechanisms

Kinetic effects alone probably cannot explain the observed stability. First, FRC formation in field-reversed theta pinches involves highly dynamic radial and axial motions. These produce significant asymmetries during formation, which have a tilt-like component. Nevertheless, the plasmas are observed to recover and settle into a quiescent state that appears to be axisymmetric. This suggests the existence of a "restoring force" that overcomes the usual overturning force. Second, even with the reduced growth rates predicted by Vlasov-fluid theory, there are a number of instances where the observed configuration lifetime is five to thirty times $1/\gamma_{tilt}$. In view of the dynamical nature of the formation few growth times should be needed in order to reach disruption.

A restoring force may arise as a result of nonstandard MHD effects, such as rotation. A trial function approach indicated that if the FRC were rotating rigidly with a drift speed (at the separatrix) of about 1.6 times the speed of sound, the tilt would be stabilized (Clemente, 1983). Recently, two-fluid effects (separate electron and ion displacement functions) were suggested to influence tilt stability (Ishida, 1987). The discussion that follows is a recent analysis in which the effects of rotation and two-fluids are clearly separated.

Both ion and electron displacements, $\vec{\xi}$ and $\vec{\xi}_e$, are included in a two fluid model. The normal mode form of the displacement appropriate for the tilt (azimuthal mode number of unity) is $\vec{\xi} = \vec{\xi}(\vec{r}_o)\exp[i(\theta-\omega t)]$, with an analogous form for $\vec{\xi}_e$. Adopting a Lagrangian description, the equation of motion becomes,

$$m_i[\ -(\omega-\Omega)^2\ n\vec{\xi} - 2(\omega-\Omega)\Omega n\ \hat{z} \times i\vec{\xi} + \Omega^2 r\ \hat{r}\nabla\cdot(n\vec{\xi})] - \vec{F}(\vec{\xi},\vec{\xi}_e) = 0 \qquad [18]$$

where $\Omega\hat{z}$ is the angular velocity vector and $\vec{F}$ is the force density. The three terms in brackets are inertia effects, which reduce to the standard MHD inertia in the limit $\Omega \to 0$. The force density is given by

$$\vec{F}(\vec{\xi},\vec{\xi}_e) \equiv \nabla\left[\vec{\xi}\cdot\nabla p + \gamma p\nabla\cdot\vec{\xi} - (\vec{\xi}-\vec{\xi}_e)\cdot\nabla p_e - \gamma p_e\nabla\cdot(\vec{\xi}-\vec{\xi}_e)\right]$$
$$-\vec{j}\times\vec{B}\,\frac{\nabla\cdot(n\vec{\xi})}{n} + \vec{j}\times\left[\nabla\times(\vec{\xi}_e\times\vec{B})\right] - en\vec{B}\times(\vec{\xi}-\vec{\xi}_e) \qquad [19]$$

Terms containing $(\vec{\xi}-\vec{\xi}_e)$, or $\vec{\xi}_e$ in place of $\vec{\xi}$ represent two-fluid effects.

It can be shown that minimizing the following functional is equivalent to solving the equation of motion (Ishida, 1987),

$$I = |\delta_i|^2(\omega-\Omega)\left(\omega-\Omega-2\mu_1\Omega-\mu_2\omega_{ci}\right) + \left[\delta_i^*\delta_e + \delta_i\delta_e^*\right](\omega-\Omega)\,\mu_2\omega_{ci}$$
$$+ |\delta_e|^2\left[\gamma_o^2 - (\omega-\Omega)\,\mu_2\omega_{ci}\right] \qquad [20]$$

Here the ion and electron displacements are assumed to have the forms, $\vec{\xi} = \delta_i\vec{\eta}$ and $\vec{\xi}_e = \delta_i\vec{\eta}$, where δ_i and δ_e are complex scalar constants, and $\vec{\eta}$ is the trial function. Also, μ_1 and μ_2 are integrals of the equilibrium state taken over the separatrix volume (for an internal mode); γ_o is the tilt growth rate for standard MHD ($\vec{\xi}_e\equiv\vec{\xi}$, $\Omega=0$), which also depends on the equilibrium, and $\omega_{ci} \equiv eB_a/m_i$ is the ion cyclotron frequency based on the reference magnetic field ($B_a = B_e$). Variations with respect to both δ_i and δ_e lead to the dispersion relation,

$$(\omega-\Omega)^2 - 2(\omega-\Omega)\left(\frac{\gamma_o^2}{2\,\mu_2\omega_{ci}} + \mu_1\Omega\right) + \gamma_o^2\left(1 + \frac{2\mu_1\Omega}{\mu_2\omega_{ci}}\right) = 0 \qquad [21]$$

Adopting a trial function similar to that found in previous studies and a particular equilibrium (Hill's vortex) allows one to calculate the integrals that comprise the factors μ_1, μ_2, and γ_o, and to find the growth rate. Figure 9 shows the growth rates for one and two fluid models: $v_A \equiv B_a/(\mu m_i n)^{1/2}$ is the Alfven speed. The one fluid case corresponds to the limit $S_* \to \infty$. Here $S_* \equiv r_s/(c/\omega_{pi})$ measures the radial plasma size (which is comparable to R/ρ_{io}). Observe that accounting for two fluids results in a new stability regime for large elongation. Also shown in Fig. 9 is the effect of rotation, which is measured by the parameter, $A \equiv \Omega r_s/v_A$. Evidently a rotational drift speed at the separatrix equal to the Alfven speed does not appreciably alter the stability.

Figure 10 shows the predicted marginal stability conditions. The large stable region on the right is the consequence of two-fluid effects, while that on the left results from the stabilization of the internal mode that occurs as low elongation. Also shown are points from long-lived experimental plasmas. Although these plasmas showed no apparent instability, most of them are well within the regime predicted to be unstable. Of course the theory is for a particular equilibrium which contains unrealistic elements: clearly more general equilibria need to be considered. In the meantime an explanation for the observed stability remains elusive.

V. TRANSPORT

Once equilibrium and stability have been assured, the important issue becomes confinement of the plasma, poloidal magnetic flux, and energy, all of which are governed by the transport properties. There are two complementary approaches to confinement, as illustrated in Fig. 11. The plasma behavior can be described on both the macroscopic and microscopic scale. On the macroscopic scale is the global behavior of the configuration (sometimes called "global transport"). This includes the plasma, poloidal flux, and energy confinement times, and the self-consistent temperature and density profiles. The confinement times can be inferred in experiments by measuring the time dependence of certain quantities (separatrix radius and length, external magnetic field, and average density at the midplane) and using the formulas, (10-12) characteristic of elongated equilibria. These measurements have been performed more or less routinely on several FRC devices. On the microscopic scale are the mechanisms which cause the transport; collisions, microturbulence, etc. This includes microstability, i.e. stability on the scale of an ion gyroradius or less. Experimental measurements of microtransport are more difficult and have only been attempted in two instances. Note that microtransport and global transport are closely interconnected. On the one hand microscopic transport determines the global transport properties of the plasma. On the other global transport, by setting the profiles, affects the transport, especially if gradient-driven microinstabilities are important.

Experimental FRCs have properties (density, temperature, size) similar to that found in theta pinch plasmas. In view of these similarities, it was natural that research into FRC transport would focus on microtransport mechanisms familiar in theta pinch lore. Consequently, a three-part picture of FRC confinement emerged. First, inside the separatrix the governing process is cross-field diffusion. The mechanism was believed to be turbulence generated by the lower-hybrid-drift (LHD) instability, as appears to be the case for ordinary theta pinches. Second,

the dissipation of poloidal magnetic flux was expected to be governed by classical (Spitzer) resistivity at the magnetic null point since theory predicts that LHD turbulence is stabilised as $B \rightarrow 0$. Finally, in the edge layer, the transport would be a combination of LHD diffusion coupled with axial "endloss" at the thermal speed. Observe that each of these statements identify particular microtransport processes.

One of the most interesting sagas of FRC research has been the process whereby the elements in the above picture of FRC confinement have proved to be faulty. The discussion that follows highlights this process.

A. Global Transport Modeling and Observations

In a global transport model, any microtransport mechanism can be assumed. This is done by using appropriate formulas for the local resistivity and thermal diffusivities. Once the self-consistent profiles are calculated, the confinement times for poloidal flux and particles are easily found. With a one-dimensional model these are given by

$$\tau_\phi = \frac{\phi_p}{2\pi}\left(rBv_D\right)^{-1}_{r=R} \qquad [22]$$

$$\tau_N = \frac{\bar{n}r_s}{2}\left(nv_D\right)^{-1}_{r=r_s} \qquad [23]$$

Here v_D is the local radial diffusion velocity given by

$$v_D = \frac{\eta_\perp}{\mu B}\frac{\partial B}{\partial r} \qquad [24]$$

where B is the axial field (1D model), and thermoelectric effects are ignored. Note that the flux confinement time is determined by the resistivity at field null (r = R) and the particle confinement is determined by the resistivity at the separatrix ($r = r_s$).

The first large computations of FRC transport were done nearly ten years ago. These included one-dimensional time-dependent models, and so-called "1-1/2D" models, i.e. 2D (r,s) equilibrium with time-dependent 1D (flux-surface-averaged) transport. The first easy-to-use analysis was a 1D particle transport model (Tuszewski, 1982). At that time the actual confinement data base from experiments consisted of only one point, which in fact was consistent with the resistivity predicted by LHD theory. Subsequently a related model was developed accounting for both particle and poloidal flux loss (Steinhauer, 1985). The model was based on a self-similarity assumption,

$$n(r,t) = n_m(t)\,\tilde{n}(u), \quad u \equiv \frac{r}{R^*(t)} - 1 \qquad [25]$$

where n_m is the density at the field null. The model was applied for a large number of cases and the results used to write approximate expressions for $\eta_\perp(r_s)$ and $\eta(R)$ in terms of τ_N, τ_ϕ, etc. In this form the model can be used as an interpretive tool to infer the resistivity from experimental observations.

The first use of this model was to show that the τ_ϕ inferred in experiments requires $\eta(R)$ to be several times larger than classical (Hoffman, 1982) Later it was applied to a substantial body of confirement data from the TRX device, as shown in Fig. 12. The dashed line is the classical resistivity for a 100 eV deuterium plasma. Electron temperatures for the experimental examples shown are believed to be 100 eV or more, so that the dashed line represents an upper bound on the classical resistivity. It is difficult to explain this anomaly on the basis of LHD turbulence, which is predicted to be stabilized near r = R .

This model as well as time-dependent 1D computations (Slough, 1984) were used to analyze the particle loss as well. Figure 13 shows the comparison between experimentally observed particle confinement time and that predicted by theory. The shaded region marked "nonlinear mode-coupling theory" represents the best theory to date on LHD-driven

transport. Evidently LHD theory predicts neither the right magnitude for τ_N, nor its correct scaling with temperature.

One of the most intriguing and peculiar results of the study has to do with the inferred resistivity profile. The gross resistivity profile, $\eta(R)/\eta_\perp(r_s)$, is plotted against $x_s \equiv r_s/r_c$ in Fig. 14. The resistivity peaks at the magnetic null (r = R) for small x_s and is peaked at the separatrix (r = r_s) for large x_s. The explanation for the correlation of profile with x_s is unknown.

B. Microtransport Theory and Observations

The important transport mechanisms includes both cross-field diffusion and, in the edge layer, the endloss mechanism.

1. Diffusion processes.

The previous discussion dealt with the inability of LHD theory to explain the loss of particles and poloidal flux. This was corroborated in a recent experiment in which the expected density fluctuations from the LHD turbulence were not observed (Carlson, 1987). Recently, several "low-frequency" modes have been proposed to explain the transport (Krall, 1987). These modes are well-known in low-β configurations such as a tokamak but have never been applied to conditions relevant to a FRC, e.g. high-β, no magnetic shear, and (in some regions) strong magnetic curvature. The likely modes include the following. 1) The high-β version of the drift dissipative mode is expected to be unstable in the moderate-β rougly straight field line regions in elongated FRCs. 2) The dissipative trapped ion mode is expected to be unstable in the strong-curvature regions near the ends of the FRC. 3) The dissipative trapped electron mode, is expected to be unstable in the high-β straight field line regions. The confinement time scaling with key plasma parameters (density, temperature, radius) for particles, poloidal flux, and energy has been estimated

(Hoffman, 1986). A preliminary investigation found these scalings to be roughly consistent with experimental observations.

2. Endloss processes.

Ideally, one might expect that the global lifetimes are determinec solely by cross-field diffusion timescales, e.g. $\tau_\perp = R^2/4\langle\eta_\perp\rangle$. For example then, one would expect $\tau_N \approx \tau$. However, the endloss time in the edge layer, $\tau_\parallel$, should be much less than $\tau_\perp$. Two consequences follow: 1) the edge layer is relatively thin (comparable to an ion gyroradius); and 2) τ_N depends on both $\tau_\perp$ and $\tau_\parallel$.

This brings us to the next unexpected observation. Given an experimental measurement of τ_N, and the assumption that $\tau_\parallel$ equals the thermal endloss time ($\ell/2$ divided by the thermal speed), then the global transport model allows one to calculate the thickness of the edge layer, δ_n. However, a survey of experimental measurements of δ_n indicates that it is several times larger than calculated in this way (Steinhauer, 1986). This corresponds to a $\tau_\parallel$ which is three to five times larger than the thermal endloss time. Several possible causes of this and related anomalies were examined. The only reasonable explanation seems to be the presence of an electrostatic potential "hill", located near the x-points at the ends of the FRC. Such a potential hill would retard the ion loss, affect the energy spectrum of the escaping ions, and make the confinement time, $\tau_\parallel$, independent of ℓ_s. All of these tendencies were detected in the experimental results. Interestingly, some of these phenomena are characteristic of mirror or tandem mirror plasmas. Collisionless mirror physics were not expected in FRC edge layers because they were thought to be too dense and collisional.

VI. SELECTED BIBLIOGRAPHY

A. Historical

T.S. Green and A.A. Newton, Phys. Fluids 9, 1386 (1966).
An early paper highlighting the loss of magnetic flux that occurs during the field-reversal phase.

A. Eberhagen and W. Grossmann, Z. Physik 248, 130 (1971).
Demonstrated FRCs lasting many Alfven transit times that did not suffer tearing instabilities.

A.G. Es'kov, et al., in Plasma Physics and Controlled Nuclear Fusion, (International Atomic Energy Agency, Vienna, 1978), p. 187.
Demonstrated long-lived FRCs by innovative formation techniques: highlighted the importance of axial compression effects.

M.N. Rosenbluth and M.N. Bussac, Nucl. Fusion 19, 489 (1979).
Identified the tilting mode as an important global instability in compact toroids: noted that it is an internal mode for elongated configurations.

W.T. Armstrong, et al., Phys. Fluids 24, 2068 (1981).
First comprehensive description of experimental results from FRC experiments (FRX-A and FRX-B). Also contains an exposition of important FRC equilibrium properties.

B. Key Proceedings and Documentary Issues

Proceedings of the US-Japan Joint Symposium on Compact Toruses and Energetic Particle Injection, Princeton Plasma Physics Laboratory, 12-14 December 1979.

Proceedings of the Third Symposium on the Physics and Technology of Compact Toroids in the Magnetic Fusion Energy Program, Los Alamos National Laboratory, Report LA-8700-C (1980).

Proceedings of the Fourth Symposium on the Physics and Technology of Compact Toroids, Lawrence Livermore National Laboratory, 27-29 October 1981.

Proceedings of the Fifth Symposium on the Physics and Technology of Compact Toroids, Mathematical Sciences Northwest, Bellevue, 16-18 November 1982.

Proceeding of the Sixth U.S. Symposium on Compact Toroid Research, Princeton Plasma Physics Laboratory, 20-23 February 1984.

Proceedings of the Seventh Symposium on the Physics and Technology of Compact Toroids in the Magnetic Fusion Energy Program, Santa Fe, Los Alamos National Laboratory, Report LA-10830-C, 21-23 May 1985.

Fusion Technology 9, number 1 (1986), special issue on compact toroid research.

Proceedings of the 8th Symposium on Compact Toroids, University of Maryland, 4-5 June 1987.

C. Important Papers by Physics Topic

1. Formation

R.D. Milroy and J.U. Brackbill, Phys. Fluids 25, 775 (1982).
The first comprehensive paper on 2D-MHD modelling of FRC formation in a theta pinch, examining many dynamical aspects of the formation.

V.V. Belikov, et al., in Plasma Physics and Controlled Nuclear Fusion Research (Proceedings of the 9th International Conference), IAEA, Vienna, 1982.
Introduced the programmed formation method.

L.C. Steinhauer, Phys. Fluids 26, 254 (1983).
The original global thermodynamic model of FRC formation.

L.C. Steinhauer, Phys. Fluids 28, 3333 (1985).
Analytical and numerical modelling of the field reversal phase.

J.T. Slough et al., in Proceedings of the Seventh Symposium on the Physics and Technology of Compact Toroids in the Magnetic Fusion Energy Program, Los Alamos National Laboratory, Report LA-10830-C (1985), p. 106.
Discussion of some of the special techniques used to improve FRC formation in a theta pinch.

A.L. Hoffman et al., Fusion Technology 9, 48 (1986).
An easy to follow simplification of the global thermodynamic formation model.

R.D. Milroy and J.T. Slough, submitted to Phys. Fluids (1987).
Polcidal flux loss and axial dynamics during the formation of a field-reversed configuration.

2. Equilibrium

R.L. Spencer and M. Tuszewski, Phys. Fluids 28, 1812 (1985).
Computational and experimental analysis of FRC equilibria.

D.J. Rej, et al., Phys. Fluids 29, 852 (1986).
Experimental and computational study of FRC translation.

3. Stability

D.C. Barnes and C.E. Seyler, in Proceedings of the US-Japan Joint Symposium on Compact Toruses and Energetic Particle Injection, Princeton, 12-14 December 1979.
Calculated the rotational stable time based on spinup driven by particle loss.

H.L. Berk, et al., Phys. Fluids 25, 473 (1982).
Stabilization of the tearing mode by a conducting wall.

Y. Aso, et al., Nucl. Fusion 22, 843 (1982).
Rotational instability is delayed by longer guide fields at the ends of the main coil, suggesting the importance of the end-shorting mechanism in governing spinup.

S. Ohi et al., Phys. Rev. Lett. 51, 1042 (1983).
First demonstration of multipole stabilization of the rotational instability.

J.L. Schwarzmeier et al., Phys. Fluids 26, 1295 (1983).
Trial function and initial value problem (linearized MHD) computations of the internal tilt instability for various equilibria.

D.S. Harned, Phys. Fluids 26, 1320 (1983).
Hybrid model of rotational instability in FRCs: predicted instability at all rotational speeds.

R.A. Clemente and J.L. Milovich, Phys. Fluids 26, 1874 (1983).
Calculated the stabilizing effect of rotation on the internal tilt mode.

T. Ishimura, Phys. Fluids 27, 2139 (1984).
MHD theory of rotational mode stabilization by multipoles.

D.C. Barnes, et al., Phys. Fluids 29, 2616 (1986).
Developed the Vlasov-fluid theory of kinetic stabilisation of the internal tilt instability.

D.J. Rej, et al., Phys. Fluids 29, 2648 (1986).
Theory and experiment on the stabilisation of the rotational mode.

A. Ishida, H. Momota, and L.C. Steinhauer, 1987, to be published.
Developed two-fluid theory of the internal tilt instability with rigid rotation: identified a new stability regime for large elongation

R.D. Milroy et al., in Proc. 8th Symposium on Compact Toroids, University of Maryland, 4-5 June 1987.
Computed the nonlinear growth of the internal tilt mode, and made preliminary investigation of the effect of rotation.

4. Transport

M. Tuszewski and R.K. Linford, Phys. Fluids 25, 765 (1982).
A quasianalytical global model of particle transport in FRCs.

A.L. Hoffman et al., Appl. Phys. Lett. 41, 31 (1982).
First reporting of anomalous (nonclassical) poloidal flux loss.

J.T. Slough et al., Nucl. Fusion 24, 1537 (1984).
First extensive comparison of experimental flux and particle confinement times with various microtransport assumptions.

L.C. Steinhauer et al., Phys. Fluids 28, 888 (1985).
Showed that lower-hybrid-drift turbulence does not explain the FRC particle and flux loss (TRX-1 device).

M. Tuszewski, et al., Phys. Fluids 29, 863 (1986).
Showed that lower-hybrid-drift turbulence does not explain the FRC particle and flux loss (FRX-C/T device).

A.L. Hoffman et al., in Plasma Physics and Controlled Nuclear Fusion Research (IAEA, Vienna, 1986).
Presents empirical confinement scaling relationships; proposes low-frequency microinstabilities as possible transport mechanisms and expresses the corresponding scaling laws.

L.C. Steinhauer, Phys. Fluids 29, 3380 (1986).
Shows the inadequacy of the MHD flow explanation for the endloss time in the edge layer; proposes an electrostatic confinement mechanism.

N.A. Krall, Phys. Fluids 30, 878 (1987).
Discussion of "low-frequency" microinstabilities that may govern the transport in FRCs.

A. Carlson, submitted to Phys. Fluids, 1987.
Laser scattering measurements which did not show the telltale fluctuations expected for LHD turbulence.

Table I

TYPICAL FRC PARAMETERS IN CURRENT EXPERIMENTS

PLASMA PARAMETERS

n - 1-5 x 10^{15} cm^{-3}	density
T_i - 100-1000 eV	ion temperature
T_e - 100-200 eV	electron temperature
$\langle\beta\rangle$ - 0.9	

PLASMA SIZE AND SHAPE

r_s - 5-10 cm	separatrix radius
ℓ_s - 30-150 cm	separatrix length
$\ell_s/2r_s$ - 3-10 cm	elongation

CONFINEMENT

τ_N - 40-150 μs	particle confinement time
$\langle\chi_e\rangle$ - 5-10 m^2/s	thermal diffusivity
$n\tau_E$ - 1-4 x 10^{11} cm^{-3} -s	

Table II

PARAMETERS OF ACTIVE THETA PINCH FRC EXPERIMENTS

	THETA PINCH COIL				TRANSLATION CHAMBER		
	r_c(cm)	ℓ_c(cm)	B_{max}(kG)	$\tau/4(\mu s)$	r_c(cm)	B(kG)	EMPHASIS
FRX-C/LSM (Los Alamos, USA)	35	200	5	12	20 (planned)	≤8	formation, translation
LSX (Spectra Technology, USA	44	400 under construction)	7	25	--	--	stability, transport
OCT (Osaka Un., JAPAN)	11	60	10	3	6.5-15	1-4	rotational stabilization, translation
PIACE (Osaka Un., JAPAN)	7.5	100	8-15	2.3	--	--	diagnostics development
NUCTE (Nihon Un., JAPAN)	8	200	10	2	--	--	rotational stabilization, formation
Bochum Un., W. GERMANY	10.5	60	30	5.8	--	--	diagnostics development
TL (Kurchatov Inst. USSR)	10	83	10	5	?	?	formation
TOR (Kurchatov Inst. USSR)	18	100	20	10	?	?	compression heating

LIST OF FIGURES

1. Characteristics of a field-reversed configuration.
2. Magnetic field plots during FRC formation in a field-reversed theta pinch.
3. Flux retention efficiency observed on TRX-1 and TRX-2.
4. Comparison of measured and predicted poloidal flux.
5. Heating intrinsic to FRC formation in TRX-2.
6. Quad-upole stabilization of rotational instability: comparison of theory and experiment.
7. Contours of constant R A_θ.
8. Reduction of internal tilt mode growth rate by kinetic effects.
9. Internal tilt growth rates for one and two fluid models, and with rotation.
10. Comparison of internal tilt mode stability predictions with experiment.
11. Confinement description approaches.
12. Anomalous flux loss in FRCs.
13. Comparison of particle confinement on TRX-1 with lower-hybrid drift theory.
14. Inferred resistivity profile.

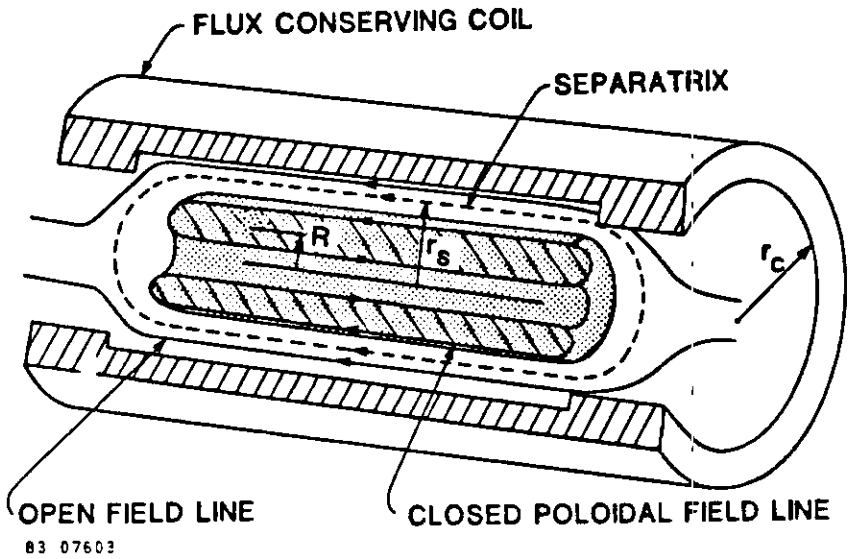

Figure 1. Characteristics of a Field Reversed Configuration

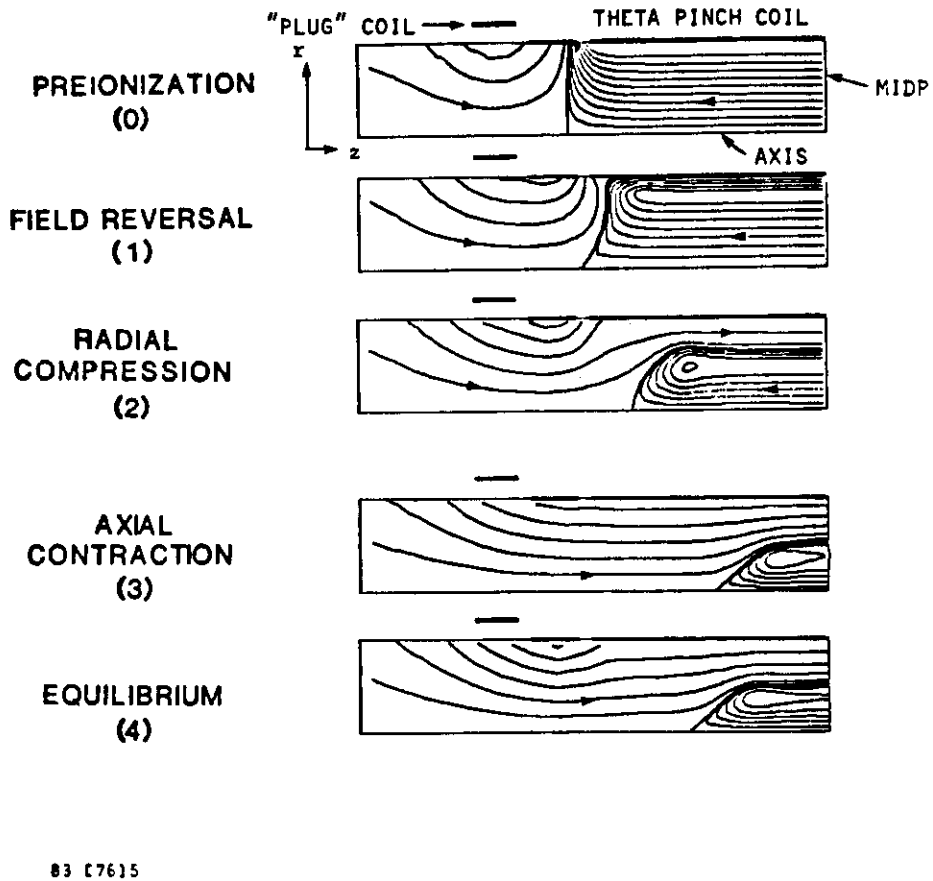

Figure 2. Magnetic field plots during FRC formation in a field-reversed theta pinch

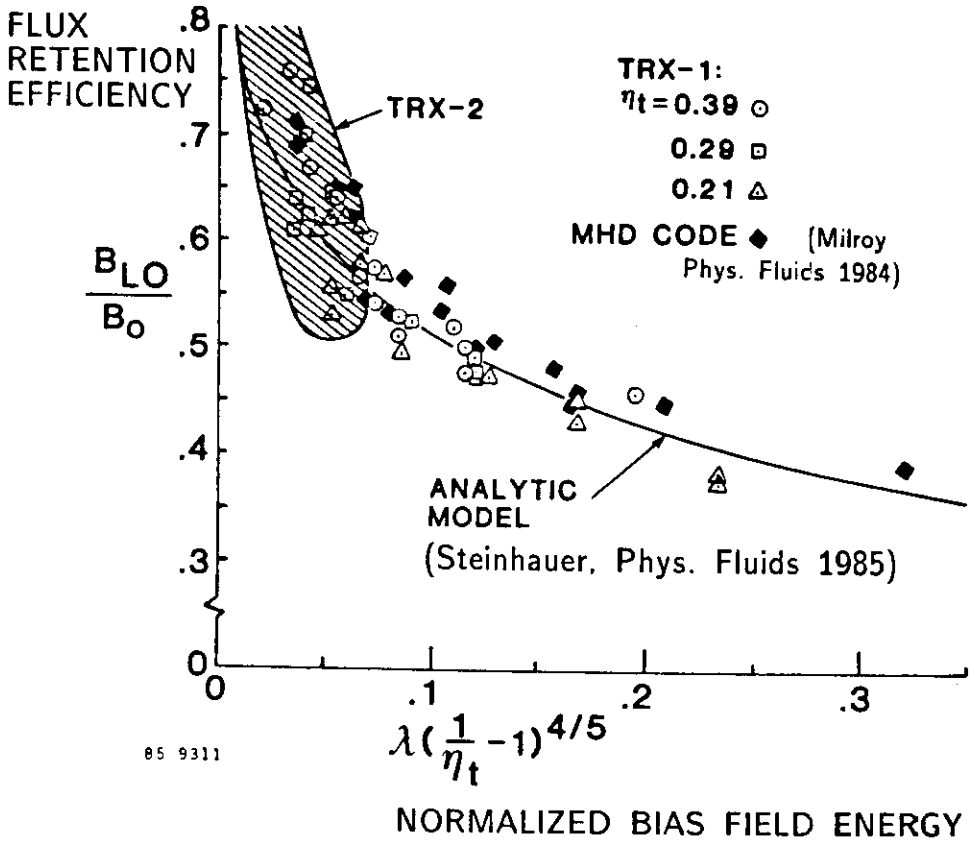

Figure 3. Flux retention efficiency observed on TRX-1 and TRX-2.

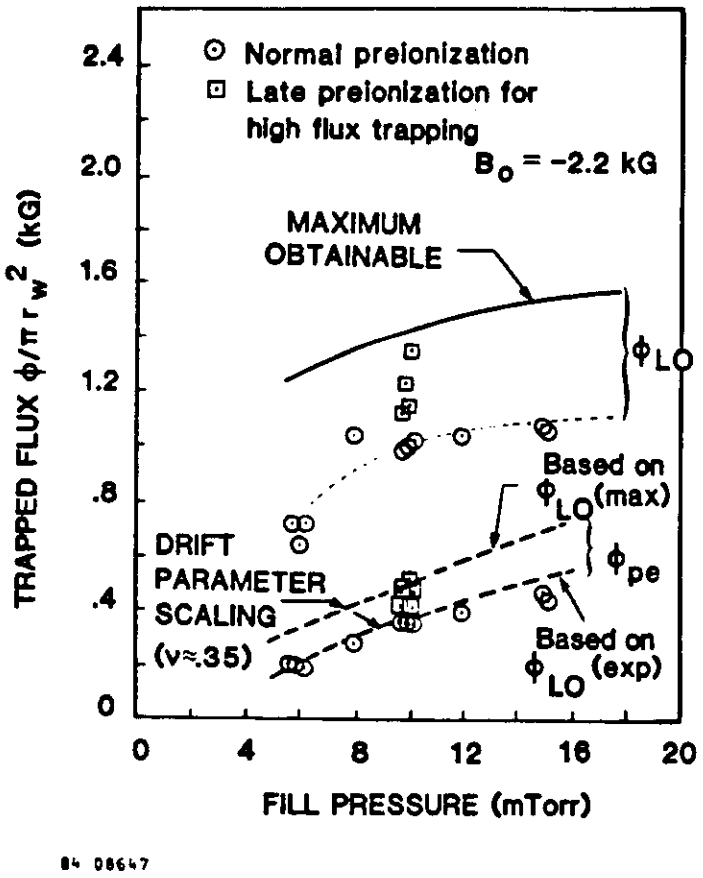

Figure 4. Comparison of measured and predicted poloidal flux.

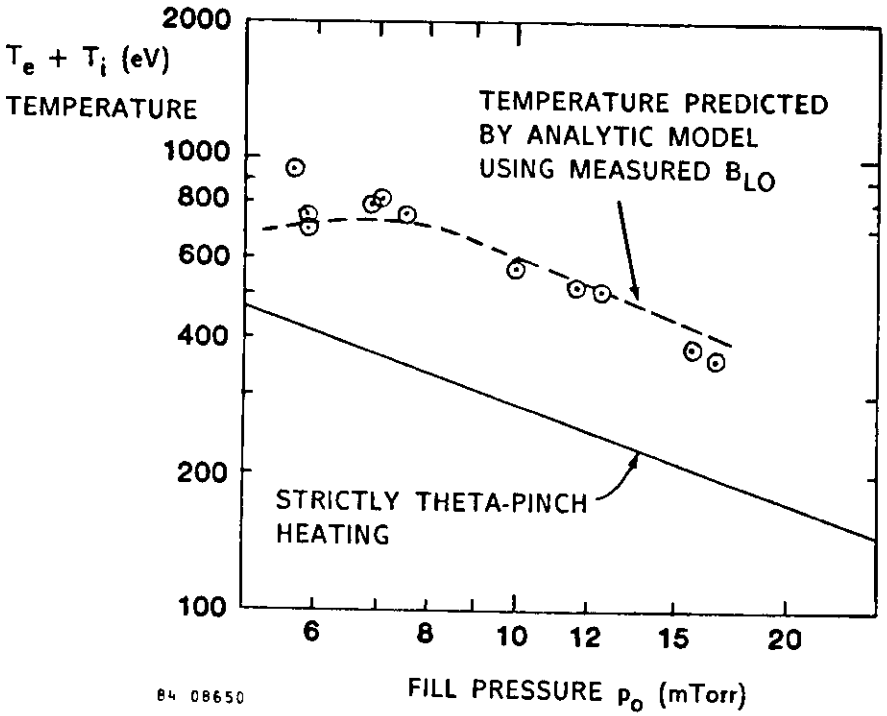

Figure 5. Heating intrinsic to FRC formation in TRX-2.

A. THEORY: hybrid code (kinetic ions, inertialess fluid electrons)

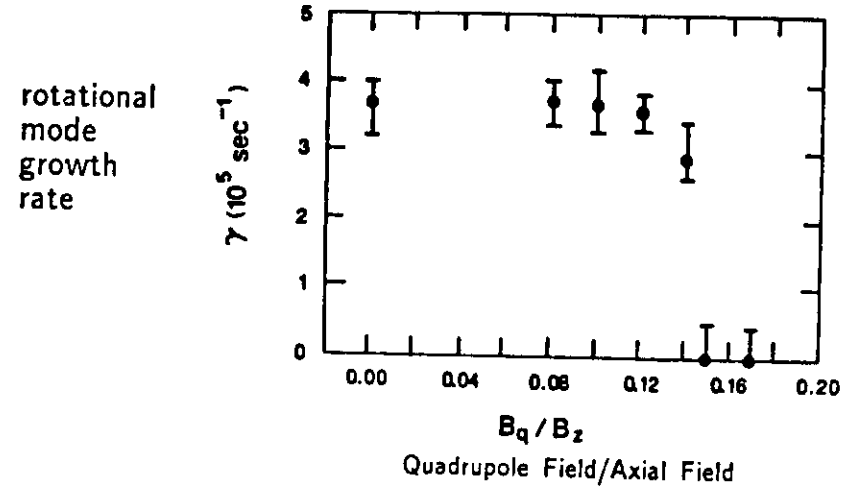

B. EXPERIMENT: FRX-C/T

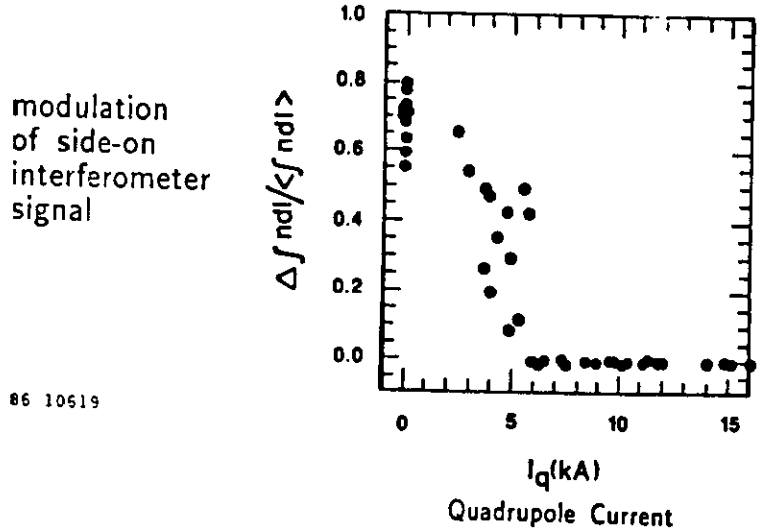

Figure 6. Quadrupole stabilization of rotational instability: Comparison of theory and experiment.

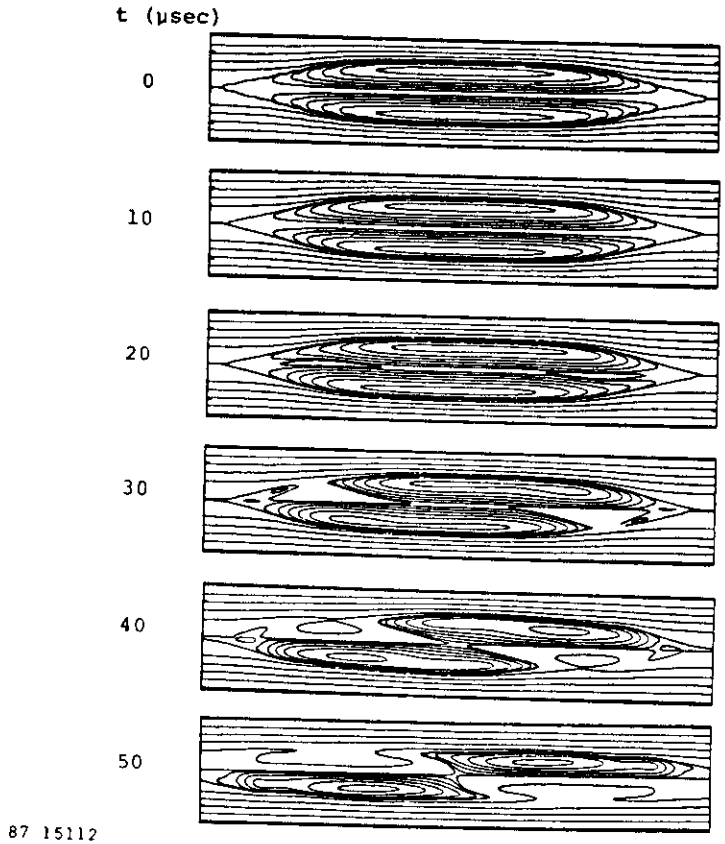

Figure 7. Contours of constant R A_θ

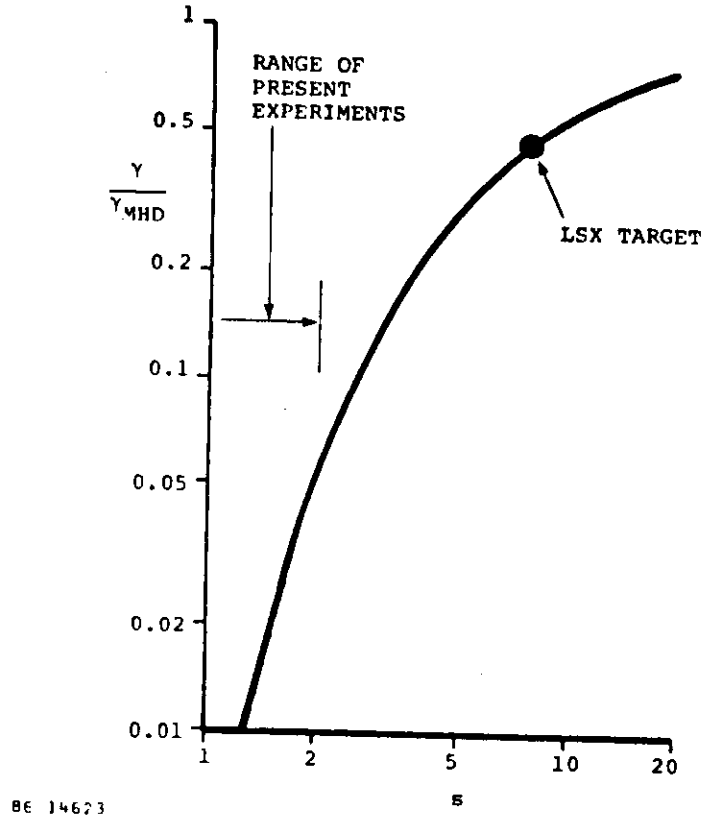

Figure 8. Reduction of internal tilt mode growth rate by kinetic effects.

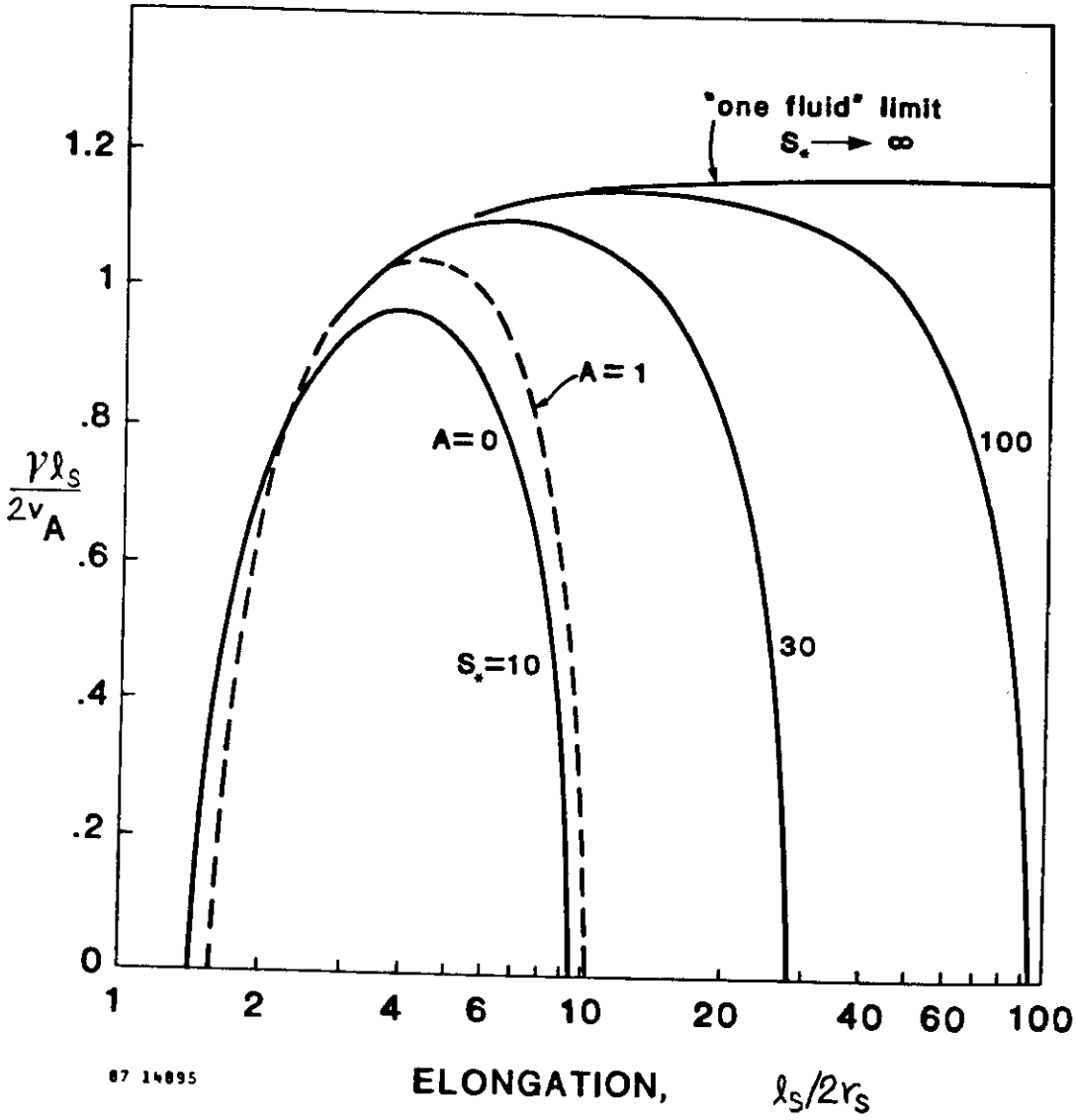

Figure 9. Internal tilt growth rates for one and two fluid models, and with rotation.

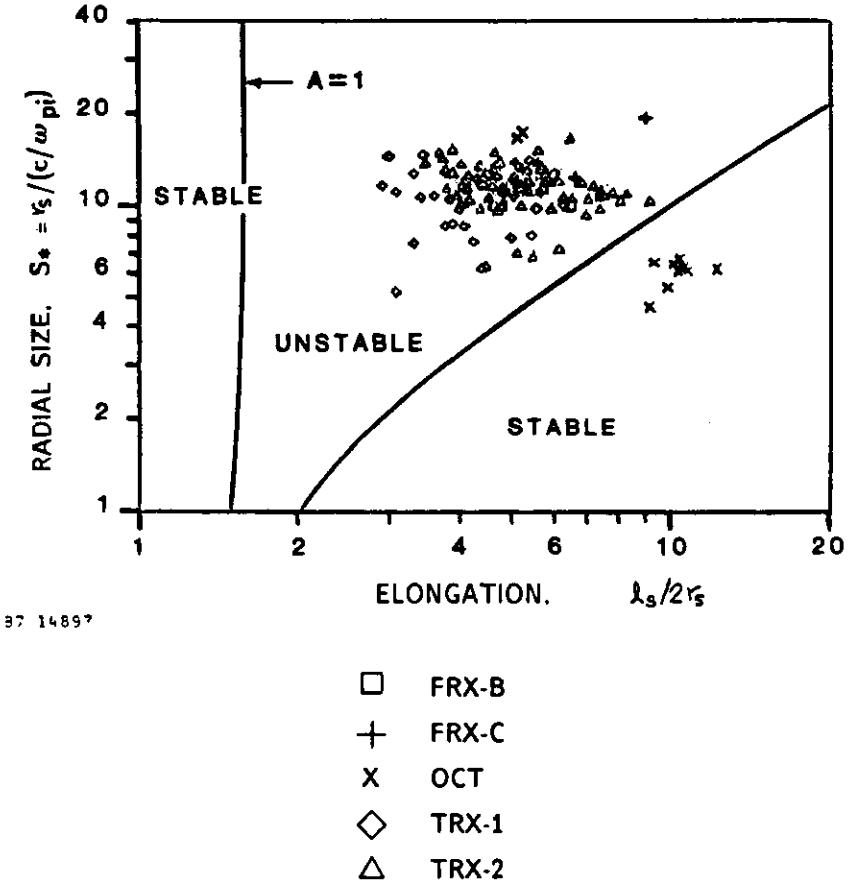

Figure 10. Comparison of internal tilt mode stability predictions with experiment.

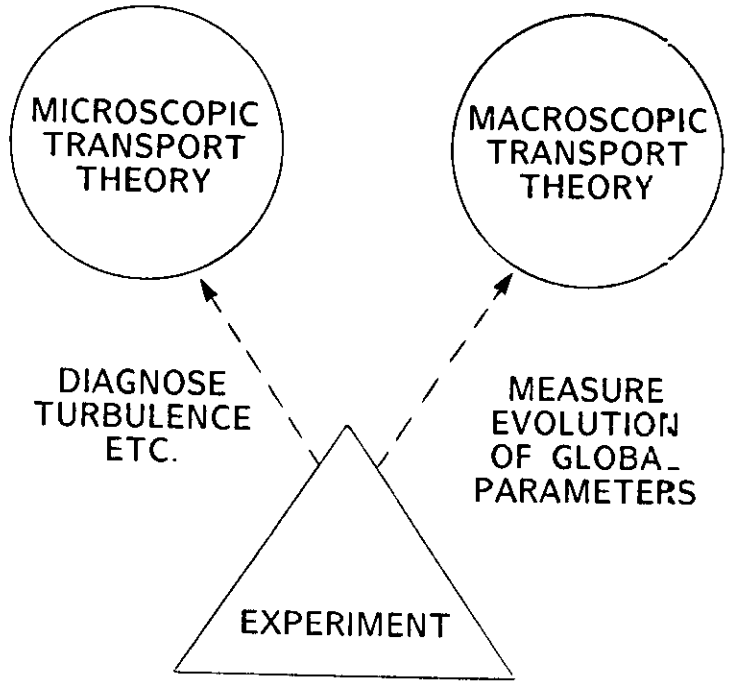

Figure 11. Confinement description approaches.

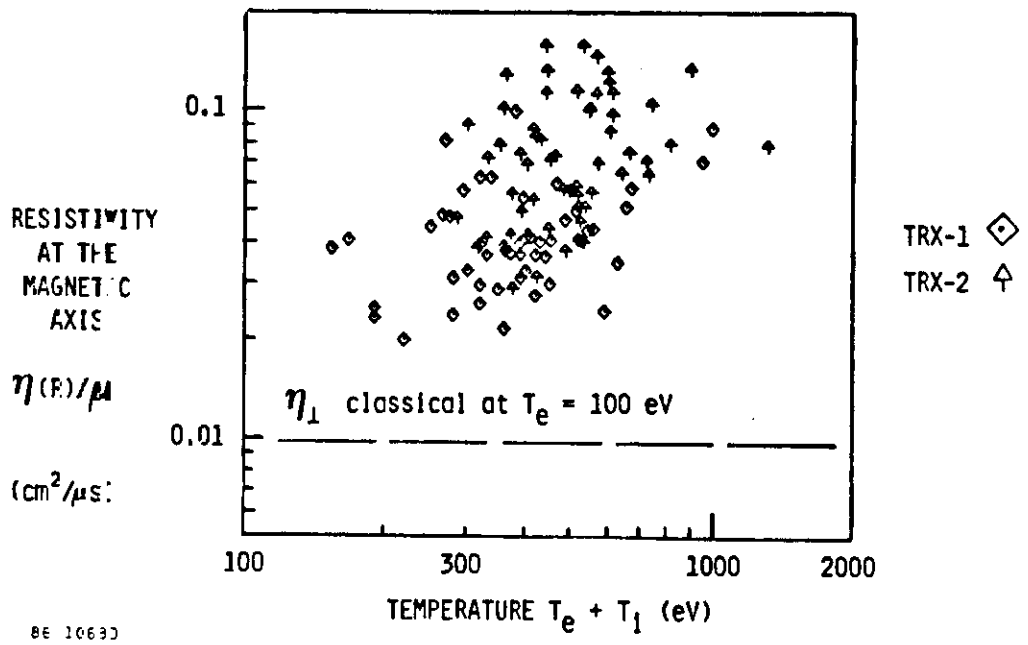

Figure 12. Anomalous flux loss in FRCs.

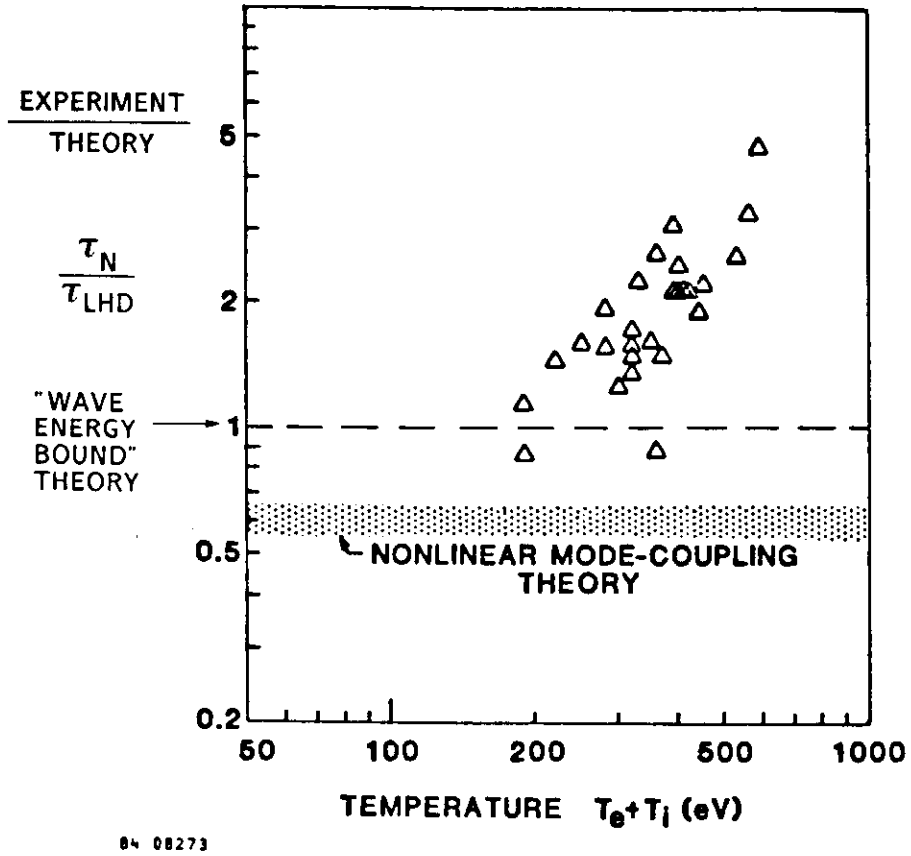

Figure 13. Comparison of particle confinement on TRX-1 with lower-hybrid drift theory.

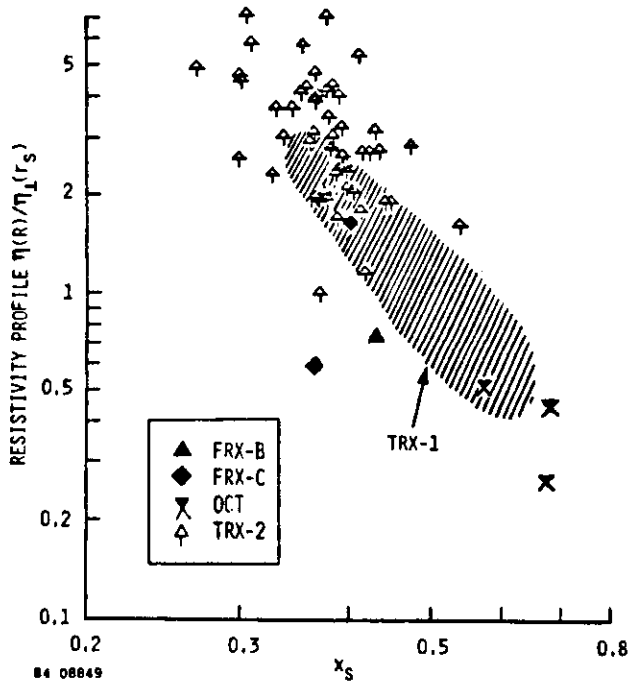

Figure 14. Inferred resistivity profile.